NATO-ADVANCED RESEARCH WORKSHOP (ARW)
"EXPLORING MULTIDISCIPLINARY APPROACHES TO CHEMICAL AND BIOLOGICAL DEFENSE",
19-23 June, 2011, Eilat ISRAEL

Fundamentals and Prediction of Persistent Agent Fate in the Environment

M.M. Sushchikh[1] , Shangshu Cai[1] , C.-H. Chang[1] , A. Lukyanov[2] and T.G. Theofanous[1]

1. Center for Risk Studies and Safety (CRSS), University of California at Santa Barbara, CA 93106
2. Department of Mathematics, University of Reading, Reading RG6 6AX, UK

Abstract. *We present first-of-a-kind experimental data that demonstrate the key physics of surface-interaction-driven, superfast diffusion at ultra-low saturations of persistent simulant agents in sand. The concept is general and applies for any substrate with multiscale surface roughness as are most, if not all environmental and operationally-relevant substrates. A mathematical model (not included due to space limitations) has been formulated on this basis and a path has been established for deriving in a predictive manner the parameters of the model from the relevant properties of the system.*

Introduction. Understanding of persistent agent fate in the environment is limited to data-fits performed on agent/substrate-specific basis, either empirically or by means of phenomenological models whose parameters bear no relation to the physics/chemistry involved. Current ATD codes used for consequence analysis are even further removed from reality by relying on phenomenology of agent distribution in a substrate that is known to be erroneous (for example, the receding-front model). Fundamental science on wetting on the other hand cannot inform because so far it has mainly dealt with ideally-structured surfaces[1], or smooth, impermeable, substrates and did not address the long-term regime as needed for persistent agents. The aim of this work is to address this scientific gap and thereby create a bridge for understanding and prediction for real environmental materials and operationally-relevant substrates.

We start from the hypothesis that the crucial process is ultra-sub-saturated transport, which is activated by multi-scale roughness, or surface open porosity (sub- micron scales), and proceeds down to molecular-level films (**Figure 1**). One implication is that traditional substrate permeability, and hydraulic conductivity (and relative-permeability-based approaches) are utterly irrelevant. Specifically, this is not a flow process but a diffusion process—as such it is driven by molecular scale liquid-solid interactions at the wetting front, while viscosity provides a resistance factor to this driving force, and slow evaporation provides the limits to how far this front can reach. Another implication is that the so-reduced problem provides a rational means for simulation in the laboratory as well as on the computer. In this paper we demonstrate this paradigm-shift for the TBP (as VX simulant)-sand system. We present first-of-a-kind Micro X-ray Computer Tomography (MicroXCT), Raman microscopy, and fluorescence-tracing data that support the stated hypothesis, we quantify spreading out to the requisite long-term, ultra-low saturations as we have found them to exist with highly persistent liquids, and we provide the means for first-principle prediction on the basis of measureable quantities.

In all experiments discussed here we use standard Ottawa (Illinois) sand with an average grain size of 250 μm, porosity of 30%, specific surface area of 0.05 m^2/g by BET, 80% attributable to

micron-scale roughness. Unless otherwise stated the liquid is tributyl phosphate (TBP). One set of experiments were done in 1D geometry by contacting slightly-"wet" sand placed in a hemispherical well, with dry sand placed inside a linear groove (**Figure 2**). The test-piece is made from PTFE stock; we have confirmed that it is prohibitive to wetting by the test liquids used. *Standard-loads* of wet sand were prepared by mixing with liquid quantities at saturations of 1, 2, 3, 4, and 5% and these were used in repeat experiments. The homogenization of mixing was finished in an ultrasound bath for at least 30 minutes. In these 1D-diffusion tests we measured front position with time by Raman spectroscopy, and in counter-part tests by fluorescence (Coumarin dye in UV). In both test series the process was followed out to many days with the test pieces left exposed to a quiescent atmospheric air; in a small box in the former, and an 2 m^3 optical enclosure in the latter. In a third series of tests all 5 standard loads and one made with 20% saturation were examined by MicroXCT. Finally, in a fourth series we carried out integral tests, with measured quantities of the liquid (11 or 88 microliters) deposited on naturally-packed sand beds, using fluorescence to trace the diffusion process. The experimental setup included an imbedded grid and a support-lowering mechanism so as to capture the granulated portion after some time of diffusion. In this last series in addition to TBP we also employed three other liquids from the organophosphate family: TCP, TBEP, and TEHP. Of these the TBEP has the most complex molecular structure. It turns out that this is of critical importance to solid-liquid molecular interactions and to the surface-diffusion mechanism. Relevant properties are summarized in **Table 1.**

Transport occurs via invisible films on grain's surface. As an initial test we detected TBP "climbing" up a dry-sand grain placed on top of a 5% standard-load sample (**Figure 3**). Grain surface morphology, and precision of locating the exact Raman-measurement spot in repeat tests are illustrated in **Figure 4**. In the 1D-diffusion tests we determined the front position as function of time (**Figure 5**), and the time-wise evolution of the front (**Figure 6**). The process was followed for up to 9 days, when only traces of liquid could be detected anywhere on the outer surface sample accessible optically. Subsequent analysis confirmed that there was no liquid present anywhere inside the sample.

The disconnected-bridge pattern. In these tests we investigate liquid distribution inside standard-load mixtures by direct microscopic 3D imaging using MicroXCT. Sample were placed in a thin-wall, 5-mm in diameter, 4-mm in depth, surface-treated ceramic cup (to render it non-wetting) and scanned for periods of 12 hours each. The three phases (sand, liquid, air) are readily visible in the analogue 3D image reconstructions and provide a qualitative insight of the scarcity and increasing isolation of liquid bridges at the contact points of sand grains at saturations of under 5%. Quantitative analysis involves an elaborate procedure on the massive amounts of data generated in a single scan (signal intensities at each of the one billion voxels—1.7 μm on the side). The result is a digital representation (using the Level-Set function) of all interfaces (**Figure 7**), which is then used to determine statistics of volume fractions, length scales and even curvatures. At low saturations the amount of liquid found in bridges is a very small fraction of

that present in the sample (**Figure 8**). The rest resides in invisible (sub-micron scale) films as revealed by the Raman tests above. The 20% saturation sample confirms that this "film phase" may contain up to an equivalent saturation of 7%. Using BET data we estimate the thickness of corresponding uniform film to be 2 μm. This can be easily configured to exist inside the sand-grain surface roughness of 10-15 μm.

Ultra-low-saturation, superfast diffusion. Counterpart to the 1D Raman spectroscopy tests, runs with fluorescence imaging (**Figure 9**) reveal a similar diffusion law (**Figure 10**). This shows that by choosing an appropriate solvent-dye combination, our fluorescence technique allows reliable detection even in this extreme sparse-liquid regime. Because of the continuous atmospheric exposure however, the liquid was depleted by evaporation somewhat faster (5 instead of 9 days), which suggests the experimental means for determining the relative roles of evaporation of highly-persistent liquids against increasing resistance to diffusion with time and viscosity in the advancing front of these microscopic films. Comparison of the data to results of simulations using a propagating-front model shows their consistency with so-called superfast diffusion kinetics.

Integral tests in 3D. In this series of tests, we follow liquid from drops (8 drops of 11 microliter each) deposited on top of sand beds using fluorescence (**Figure 11**). The drop is first found to spread in the known manner, but after about 2 days, at a point where the average saturation drops to below 5% we observe a rather sharp change to a (diffusion) law with a much smaller rate constant (**Figure 12**). While the first portion matches quite well the spreading law found in similar tests using VX^2, the latter part was not known and therefore was not followed in those VX-tests, so it remains unknown whether TBP is a good simulant in this regime as well. At the end of the test, lowering the support revealed (**Figure 11**, bottom line) that the sand over the "wet" area had lost the cohesiveness normally expected and found in wet sand, which is another perhaps more tangible indication of this diffusion regime identified here. An initial exploration of the diffusion intricacies in this regime was made by similar 3D experiments carried out with single 11 microliter drops of TBP, TCP, TBEP, and TEHP placed on top of naturally-packed beds of sand (**Figure 13**). Notable are: (a) At five days the more persistent liquids (Table 1) continue to diffuse, while TBP is already arrested, (b) Right from the start, TBEP exhibits very low expansion, even in the early, "normal-spreading" portion, even though nothing in its physical properties (viscosity, surface tension, contact angle on smooth glass) singles it out from the other organophosphates used. Noting that TBEP has extra oxygen atoms embedded into the hydrocarbon branches we attribute its behavior to (molecular) surface interactions with the silicate-based material of sand grains. This is a subject of ongoing investigations.

Conclusions.

1. The persistence of extremely low vapor pressure liquids in the environment is controlled by a diffusion-like process that is activated by molecular-scale processes at the fronts of

microscopic films that propagate inside open virtual channels created by surface roughness.

2. The propagation process is resisted by liquid viscosity, and the extent of it is eventually limited by the vapor pressure of the liquid agent.
3. Fluorescence, Raman spectroscopy, and MicroXCT provide a complementary array of measurement methods that have been demonstrated to meet the needs for quantification in this regime.

References

1. D. Quere, "Wetting and Roughness", *Annu. Rev. Mater. Res.* **38**, 71-99 (2008).

2. B. Markicevic, T.G. D'Onofrio, H.K. Navaz, "On spread extent of sessile droplet into porous medium: Numerical solution and comparisons with experiments", Phys. Fluids, **22**, 012103 (2010).

Acknowledgements

This work is supported by the Joint Science and Technology Office, Defense Threat Reduction Agency (JSTO/DTRA), Threat Agent Science (TAS). Drs. F. Handler, J. Kaufman, and S. Paikoff were instrumental in the pursuit of this work.

Tables and Figures to be inserted into the text:

Table 1. Properties of organophosphates used in this study (at 25^0 C).

Name	Molecular formula	M.W. (a.m.u.)	Vapor pressure (Pa)	Surface tension (mN/m)	Kinematic Viscosity (m^2/s)
TBP	$(CH_3(CH_2)_3O)_3PO$	266.31	$1.3\cdot10^{-1}$	28	$3.5\cdot10^{-6}$
TBEP	$[CH_3(CH_2)_3OCH_2CH_2O]_3P(O)$	398.47	$3.3\cdot10^{-6}$	31.5	$12\cdot10^{-6}$
TEHP	$[CH_3(CH_2)_3CH(C_2H_5)CH_2O]_3P(O)$	434.63	$1.1\cdot10^{-5}$	29	$15\cdot10^{-6}$
TCP	$(CH_3C_6H_4O)_3PO$	368.36	$8\cdot10^{-5}$	42.5	$>18\cdot10^{-6}$

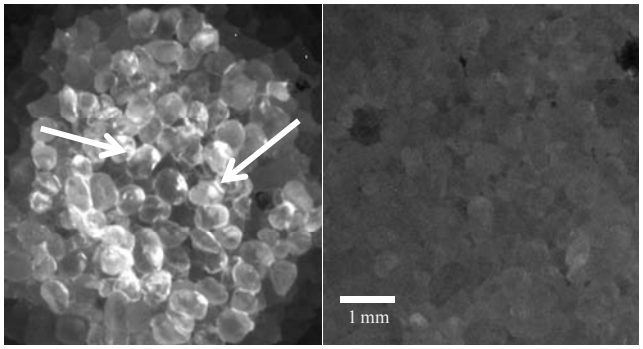

Fig. 1. Fluorescence image of TBEP (left) and TBP (right) after diffusing in sand for 4 days. TBEP exhibits slow diffusion (see below) and significant amount of it stays in liquid bridges at grain contacts. TBP diffused beyond the liquid-bridge regime and is in the form of an otherwise invisible film on the sand-grain roughness.

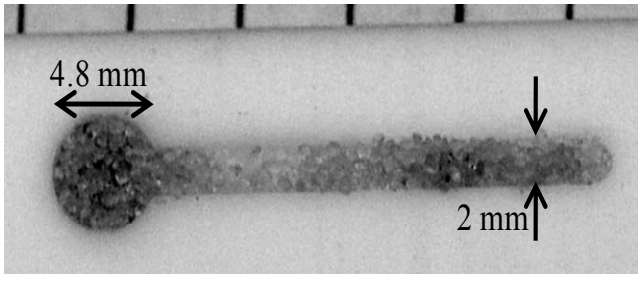

Fig. 2. Geometry of the 1D-spreading experiments. A hemispherical well opens into a rectangular groove (20×2×1 mm). At time zero the well is filled with a standard load and the groove is filled with dry sand in a way that establishes contact with the load.

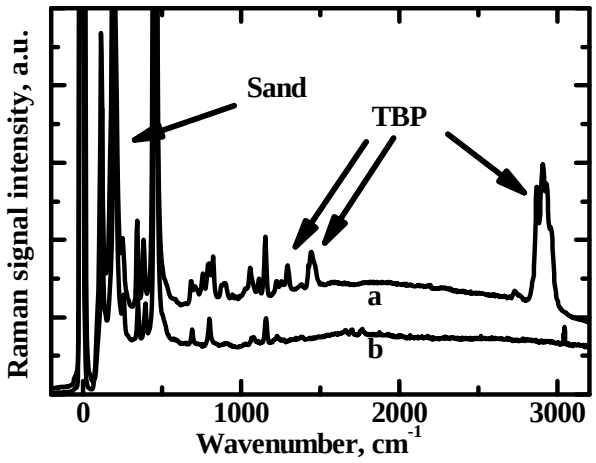

Fig. 3. Raman spectra of TBP on a sand grain surface (a), in comparison to dry-sand spectra (b).

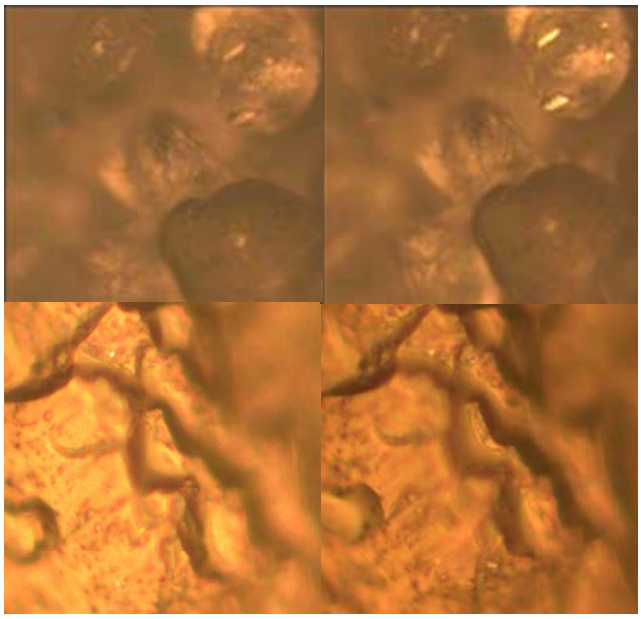

Fig. 4. The left two photos were taken at the day 2 and the right two photos were taken at day 5. Top photos at lower magnification (5×) were used for locating the same grain and then higher magnification (50×) was used to position at same spot on the grain surface. The high-resolution images cover a region of approximately 25×25 microns.

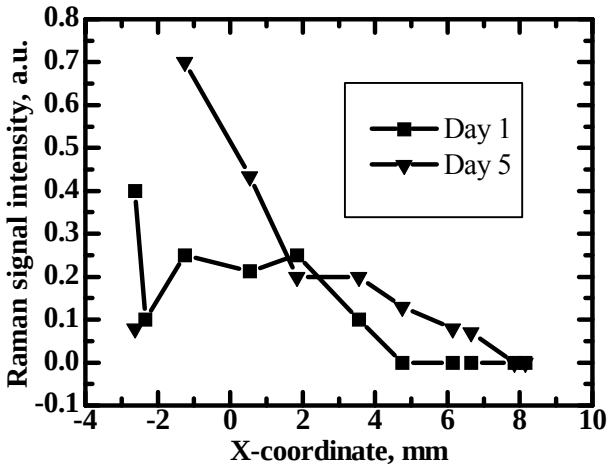

Fig. 5. Raman signal intensities at same spots on sand grains. The last non-zero value to the right indicates the position of the liquid film front. The signal intensity has no quantitative significance other than TBP presence.

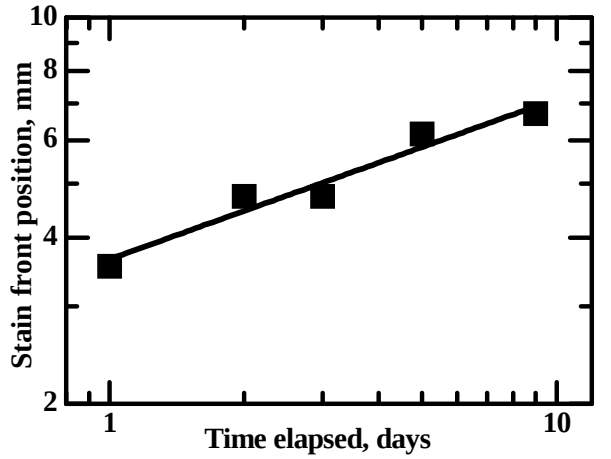

Fig. 6. The diffusion kinetics of TBP on sand. Initial saturation of the wet portion of sand was 5%. The slope of the linear fit is 0.29+-0.04.

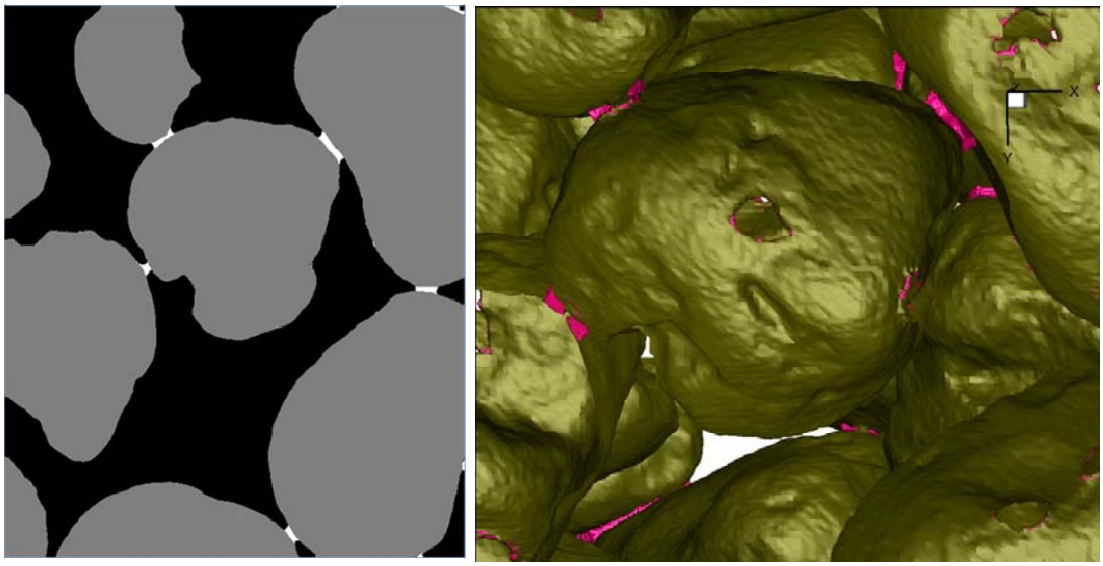

Fig. 7. MicroXCT images of sand, air and TBP found in a 3% standard load. Left: a slice showing liquid (white), sand (grey) and air (black). Right: A Level-Let-based reconstruction of the surfaces in 3D.

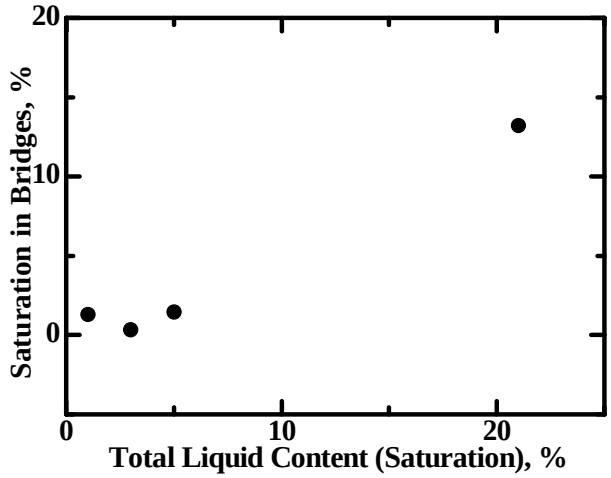

Fig. 8. Amount of TBP found in liquid bridges as found by MicroXCT over an array of standard loads.

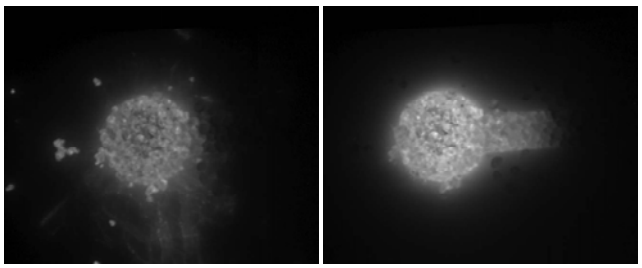

Fig. 9. Monitoring of TBP propagating in sand by fluorescence. The image on the right was taken five days later. Standard load 5%.

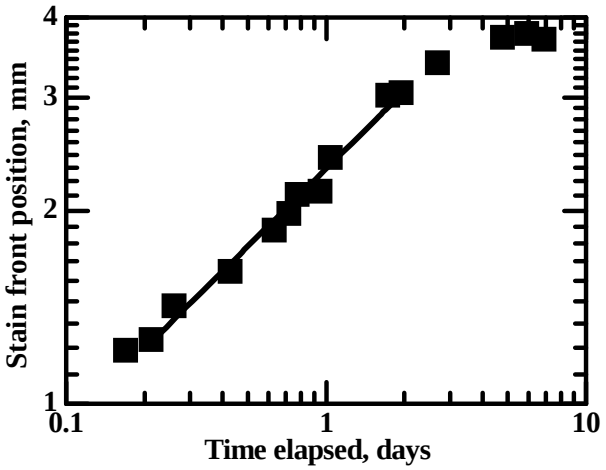

Fig. 10. The diffusion kinetics of TBP on sand. The position of the film front was determined as the edge of fluorescing area. Standard load 5%. The slope of the linear fit is 0.40+-0.02.

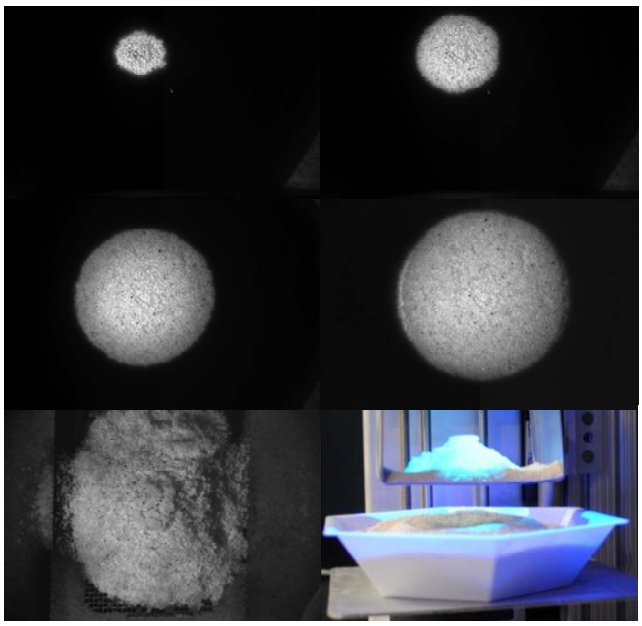

Fig. 11. Top two rows: monitoring of TBP front on sand by fluorescence. The images were taken at 0, 0.2, 1.7 and 7 days. Bottom row: crumbling of TBP-infected sand volume upon removal of the support on day nine.

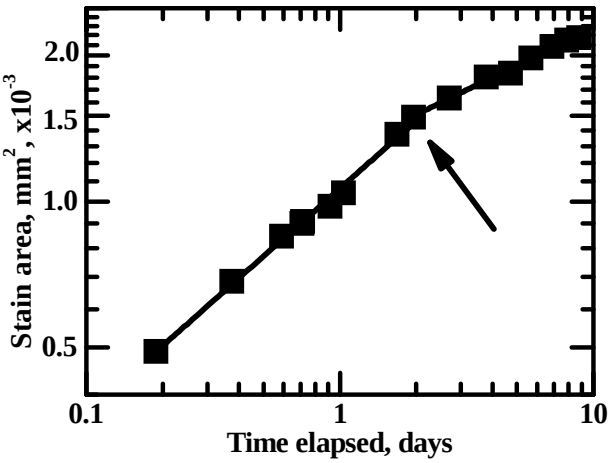

Fig. 12. The diffusion kinetics of TBP on sand in an integral 3D setting. Up to two days the slope is 0.46 then the regime changes exhibiting a slope of 0.31.

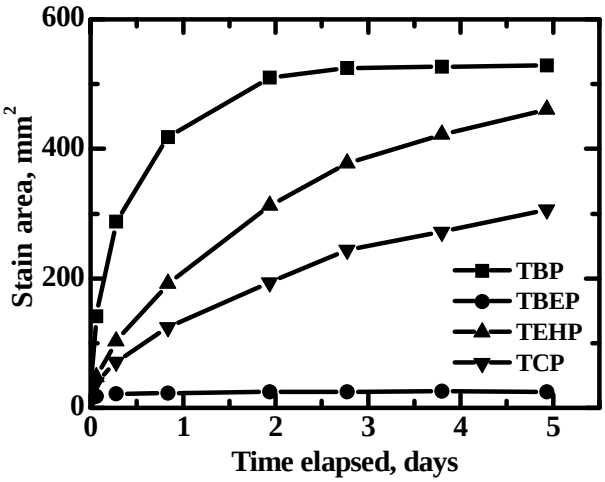

Fig. 13. Diffusion kinetics of four different organophosphates.